Versatile Poly(3,4-ethylenedioxythiophene)

Polyelectrolytes for Bioelectronics by Incorporation of an Activated Ester

Joshua Tropp, Abijeet S. Mehta, Xudong Ji, Abhijith Surendran, Ruiheng Wu, Emily A. Schafer Manideep M. Reddy, Shiv P. Patel, Anthony J. Petty, II, and Jonathan Rivnay*

Department of Biomedical Engineering, Center for Advanced Regenerative Engineering, Simpson Querrey Institute, Northwestern University, Evanston, Illinois 60208, United States

ABSTRACT. The field of bioelectronics leverages the optoelectronic properties of synthetic materials to interface with living systems. These applications require materials that are conductive, aqueous processible, biocompatible, and can be chemically modified for biofunctionalization. While conjugated polymers and polyelectrolytes have been reported that demonstrate several of these features, materials that offer each of these properties simultaneously are rare. Here, we developed copolymers of anionic polyelectrolyte poly(4-(2,3-dihydrothieno[3,4-b][1,4]dioxin-2-ylmethoxy)-butane-1-sulfonic acid sodium salt (PEDOT-S), containing structural units with amine-reactive NHS-esters. The reported PEDOT-NHS copolymers demonstrate water-solubility and electrical conductivities similar to previously reported PEDOT-S, as well as the ability to bind important amine-rich biomaterials. Furthermore, the PEDOT-NHS copolymers were biocompatible and hemocompatible, and

therefore show promise for next-generation bioelectronic and regenerative engineering applications.

1. INTRODUCTION

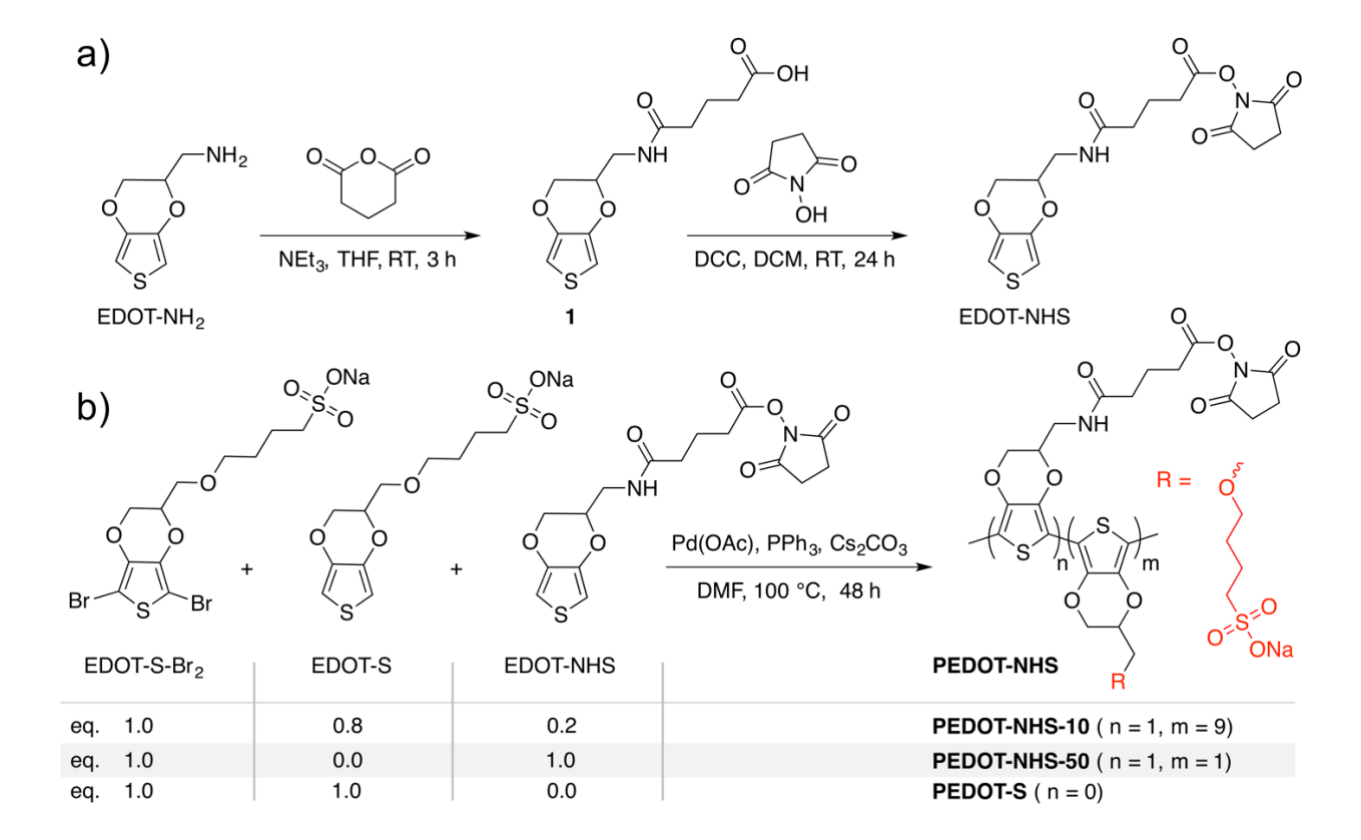
Recent advancements in bioelectronics have offered soft, tunable, biocompatible, and electroactive organic materials to interface living organisms with electronic devices. ¹⁻⁵ Such biomaterials have found utility within scaffolds for tissue engineering and regenerative medicine, ⁶⁻⁸ where a combination of active (mixed ionic and electronic charge transport) and passive (surface chemistry, morphology, mechanics) properties can restore, maintain, or improve tissue function. ⁹ Conductive biomaterials are generally designed through the incorporation of an electroactive filler (conjugated polymer, carbon nanotube, metal nanowire) into an insulating biocompatible polymer matrix. ¹⁰⁻¹¹ Conjugated polymers (CPs) have been used to great effect in bioelectronics and tissue engineering in particular due to their biocompatibility, possibility of unique form factors, and chemically tunable structures for the promotion of mixed conduction. ⁹ unique form factors, and chemically tunable structures for the promotion of mixed conduction. ⁹ to successful application within a bioelectronic technology, CPs with aqueous solubility, sites for covalent modification, electroactivity, and biocompatibility are generally required.

Such strict and specific requirements have given way to a large body of work focused on synthetically tailoring CPs for particular bioelectronic applications. Derivatives/composites of poly(3,4-ethylenedioxythiophene) (PEDOT) have been thoroughly utilized, in particular, for biointerfacing due to their favorable conductivity, electrochemical stability, and biocompatibility.^{11, 16} Functional derivatives of PEDOT have been synthetically designed with side chains to enable aqueous processability, ¹⁷⁻¹⁸ enhanced surface adhesion, ¹⁹ or

postpolymerization modification; however few materials display each of these features simultaneously.²⁰ Particularly for applications within hydrogels, the CP cannot be easily electropolymerized on the non-conductive, tortuous surface and must be incorporated via aqueous solution to enable swelling of the biomaterial for monomer/polymer ingress – thus limiting the utility of the majority of available PEDOT derivatives. While commercial **PEDOT:PSS** has been widely explored for sensing and stimulation as a thin film coating, and as a functional surface to affect cell and tissue proceesses,²¹⁻²³ its use often requires various low molecular weight additives,²⁴ is limited in its range of usable concentrations, and lacks both coating uniformity and functionalization capacitity.^{16, 25}

Self-doped, sulfonated polythiophenes such as poly(4-(2,3-dihydro-thieno[3,4b][1,4]dioxin-2-ylmethoxy)-butane-1-sulfonic acid sodium salt (PEDOT-S) have been demonstrated as viable alternatives to PEDOT:PSS for bioelectronic applications due to their enhanced solution processability, relatively high conductivity without the need of external additives/dopants, and biocompatibility. 15, 18, 26 While significant efforts have been made to synthesize and boost the conductivity of **PEDOT-S**, ²⁶⁻²⁷ the polymer lacks a chemical handle for (bio)functionalization, limiting its versatility in bioelectronics. Here, we present a synthetic strategy to incorporate a functional handle into **PEDOT-S** using a *N*-hydroxysuccinimide (NHS) activated monomer. Direct (hetero)arylation polymerization (DHAP) was utilized to systematically increase the loading of the NHS-activated structural unit (EDOT-NHS) within the polymer backbone to afford two copolymers PEDOT-NHS-10 and PEDOT-NHS-50 with 10% and 50% incorporation of EDOT-NHS, respectively. Both the optical and electrochemical properties of each polymer were investigated, which mirrored the behavior of PEDOT-S even at relatively high loadings (50%) of EDOT-NHS. The in vitro biocompatibility to each polymer

was also investigated, a material property often ignored when developing materials for bioelectronic applications; PEDOT-NHS copolymers demonstrated both biocompatibility and hemocompatibility. Incorporation of EDOT-NHS into the sulfonated polythiophene enabled amine-reactive functionalization, which was demonstrated through the covalent modification of gelatin, a biomaterial regularly utilized for tissue engineering. Taken together the reported polymers demonstrate water solubility, handles for post-polymerization modification, electroactivity, and biocompatibility, a combination that is not commonly achievable in the organic bioelectronic community.



Scheme 1. Synthesis of (a) EDOT-NHS and (b) poly[(EDOT-NHS)-co-(EDOT-S)] (PEDOT-NHS) copolymers and **PEDOT-S**.

2. EXPERIMENTAL SECTION

All manipulations of air and/or moisture sensitive compounds were performed under an inert atmosphere using standard glove box and Schlenk techniques. Reagents for polymer synthesis, unless otherwise specified, were purchased from Sigma-Aldrich and used without further purification. Deuterated solvents (CDCl₃ and CD₃OD) were purchased from Cambridge Isotopes Labs and used as received. Palladium (II) acetate was purchased from Strem Chemicals and used (2,3-Dihydrothieno[3,4-b][1,4]dioxin-2-yl)methanamine,²⁸ received. 4-(2,3as Dihydrothieno[3,4-b][1,4]dioxin-2-yl-methoxy)-1-butanesulfonic acid, sodium salt,²⁹ 4-[(5,7dibromo-2,3-dihydrothieno[3,4-b]-1,4-dioxin-2-yl)methoxy]-1-butanesulfonic acid. sodium salt,³⁰ and **PEDOT-S**,¹⁸ were prepared according to previously reported procedures. ¹H and ¹³C NMR spectra were collected on a Bruker Ascend 600 MHz spectrometer and chemical shifts, δ (ppm) were referenced to the residual solvent impurity peak of the given solvent. Data reported as: s = singlet, d = doublet, t = triplet, m = multiplet, br = broad; coupling constant(s), J are given in Hz. Flash chromatography was performed on a Teledyne Isco Combiflash Purification System using RediSep f prepacked columns. Small molecule molecular weight and formula determination were performed using an Agilent 6545 Q-TOF high resolution Mass Spectrometer using an Electro Spray Ionization (ESI) source and coupled to an Agilent 1200 series LC system. Analysis was performed using direct injection with methanol as the solvent. Attenuated total reflectance Fourier transform infrared spectroscopy was performed using a Thermo Scientific Nicolet IS10 spectrometer.

2.1. 5-(((2,3-dihydrothieno[3,4-b][1,4]dioxin-2-yl)methyl)amino)-5-oxopentanoic acid (1). (2,3-Dihydrothieno[3,4-b][1,4]dioxin-2-yl)methanamine (2.67 g, 15.6 mmol), glutaric anhydride (1.96 g, 17.2 mmol), and triethylamine (2.4 mL, 17.2 mmol) were dissolved in anhydrous THF

(50 mL) under nitrogen. The resulting mixture was stirred at room temperature for 12 h. The reaction mixture was poured into ether and extracted with 10 % Na₂CO₃. The aqueous layer was removed, acidified to pH ~ 1-2 with HCl, and extracted with ether. Volatiles were removed in vacuo, and the purification was accomplished by flash chromatography using DCM/methanol gradient affording, 3.32 g of a colorless oil (11.6 mmol, 75%). ¹H NMR (600 MHz, CDCl₃): δ 6.34 (2H, s), 4.31-4.16 (2H, m), 3.96-3.87 (1H, m), 3.71-3.61 (1H, m), 3.51-3.42 (1H, m), 2.44 (2H, t, J = 7.1 Hz), 2.32 (2H, t, J = 7.4 Hz), 1.99 (2H, p, J = 7.2 Hz). ¹³C NMR (151 MHz, CDCl₃): δ 177.85, 172.92, 141.40, 141.22, 100.18, 100.05, 72.73, 66.37, 39.72, 35.25, 32.96, 20.67, 19.83. HRMS (ESI) (m/z): [M-H]⁻ calcd for C₁₂H₁₅NO₅S: 284.060, found: 284.060.

2.2. 2,5-dioxopyrrolidin-1-yl 5-(((2,3-dihydrothieno[3,4-b)[1,4]dioxin-2-yl)methyl)amino)-5-oxopentanoate (EDOT-NHS). 5-(((2,3-dihydrothieno[3,4-b)[1,4]dioxin-2-yl)methyl)amino)-5-oxopentanoic acid 1 (3.12 g, 10.9 mmol), N-hydroxysuccinimide (1.40 g, 12.2 mmol), and N,N'-dicyclohexylcarbodiimide (2.54 g, 12.3 mmol) were dissolved in DCM (75 mL) under nitrogen. The resulting mixture was stirred at room temperature overnight. The suspension was filtered through a Buchner funnel and washed with DCM. The resulting white solid was washed with acetonitrile, and the supernatant was concentrated by rotary evaporation to afford a white solid. The solid was crystallized using DCM/hexanes, and recrystallized using acetone/hexanes affording, 2.61 g of a white solid (6.8 mmol, 63%). 1 H NMR (600 MHz, CD₃OD): δ 8.12 (1H, t, J = 5.7 Hz), 6.53 (2H, s), 4.24-4.08 (2H, m), 3.92-3.79 (1H, m), 2.77 (4H, br), 2.67 (2H, t, J = 7.4 Hz), 2.21 (2H, t, J = 7.3 Hz), 1.81 (2H, m). 13 C NMR (151 MHz, CDCl₃): δ 172.31, 169.37, 168.41, 141.46, 99.99, 99.68, 72.57, 66.32, 39.59, 34.27, 30.01, 25.71, 20.88. HRMS (ESI) (m/z): [M+H]+ calcd for C₁₆H₁₈N₂O₇S: 383.090, found: 383.091.

- 2.3. PEDOT-NHS-10. A reaction vial was loaded with EDOT-NHS (58.0 mg, 0.152 mmol), EDOT-S (200 mg, 0.606 mmol), and EDOT-S-Br₂ (371 mg, 0.760 mmol). The vial was brought inside a glove box and triphenylphosphine (43.0 mg, 0.164 mmol), cesium carbonate (520.0 mg, 0.160 mmol), Pd(OAc)₂ (17.0 mg, 0.076 mmol) and 5.0 mL of anhydrous DMF were added. The tube was sealed, and the mixture was stirred at 100 °C for 48 h. After this time the reaction was allowed to cool leaving a solid purple material. Excess solvent was decanted. The residual solid was dissolved in 2 mL of water and precipitated into acetone. The purple solid was washed with acetone by Soxhlet extraction overnight, dialyzed against water for 72 h using a 3 kDa MWCO bag, and dried via lyophilization for 72 h to afford 437 mg of polymer. *Polymer doping*: A reaction vial was loaded with the purple solid (200 mg), DI H₂O (8 mL), and an aqueous ammonium persulfate solution (0.545 mL, 1.24 M). The solution was stirred at room temperature for 10 min and precipitated into acetone. The blue solid was washed with acetone and dried under nitrogen.
- **2.4. PEDOT-NHS-50.** A reaction vial was loaded with EDOT-NHS (117.4 mg, 0.307 mmol), and EDOT-S-Br₂ (150 mg, 0.307 mmol). The vial was brought inside a glove box and triphenylphosphine (17.4 mg, 0.066 mmol), cesium carbonate (210.0 mg, 0.065 mmol), Pd(OAc)₂ (6.9 mg, 0.031 mmol) and 2.0 mL of anhydrous DMF were added. The tube was sealed, and the mixture was stirred at 100 °C for 48 h. After this time the reaction was allowed to cool leaving a solid purple material. Excess solvent was decanted. The residual solid was dissolved in 2 mL of water and precipitated into acetone. The purple solid was washed with acetone by Soxhlet extraction overnight, dialyzed against water for 72 h using a 3 kDa MWCO bag, and dried via lyophilization for 72 h to afford 520 mg of polymer. *Polymer doping*: A reaction vial was loaded with the purple solid (200 mg), DI H₂O (8 mL), and an aqueous

ammonium persulfate solution (0.545 mL, 1.24 M). The solution was stirred at room temperature for 10 min and precipitated into acetone. The blue solid was washed with acetone and dried under nitrogen.

2.5. X-ray Fluorescence. X-ray fluorescence spectroscopy was performed in a Xenemetrix Ex-Calibur EX-2600 spectrometer equipped with an Rh X-ray tube and a silicon energy-dispersive detector. Each solid sample was placed in a plastic cup and powder was supported on a 6 μ m Mylar film. Data collection was performed under vacuum and at room temperature. X-ray tube was operated at 30 keV and 100 μ A, and fluorescence spectra were collected for 60 s. No filter was used between the detector and sample and L-lines of Rh-radiation were visible in the collected spectra. Relative sulfur analysis was performed by integrating the fluorescence of the $K_{\alpha 1}$ transition for sulfur at ~2.3 keV of each material. Samples were compared under the same excitation settings and collected fluorescence was normalized by the mass of each sample.

2.6. Electrochemical and Electrical Analysis. Cyclic voltammograms were recorded using a standard three-electrode setup connected to an Ivium potentiostat. A platinum mesh (Sigma-Aldrich) and a Ag/AgCl electrode (Warner Instruments E202) were used as the counter and reference electrodes respectively. The polymers were deposited by spin-coating from aqueous solutions (20 mg mL⁻¹) at 600 rpm on ITO-coated glass substrates. The measurements were carried out in anhydrous 100 mM TBAPF₆ solution with a scan rate of 10 mV s⁻¹. Spectroelectrochemical measurements were carried out simultaneously using an OceanOptics USV 2000+ spectrometer, which collected the transmitted light through a quartz cuvette from a tungsten lamp used as a probe light source. Potentials are reported vs Fc/Fc⁺ using the half-wave potential of ferrocene acquired under the same conditions. Experiments were performed in acetonitrile rather than aqueous electrolyte to avoid the need for crosslinking to stabilize the film.

Four-point conductivity measurements were performed using a Lucas Labs Pro4 four-point probe head with a Keithley 2400 source meter according to previously reported procedures.²⁶ Aqueous solutions of doped polymer (20 mg mL⁻¹) were sonicated via horn sonication, passed through a 0.45 µm cellulose acetate syringe filter, and spin-coated onto glass substrates at 600 rpm. Each substrate was dried at 55 °C. Samples were measured in triplicate, and the average film thickness was determined via profilometry.

2.7 In Vitro Cytotoxicity. In vitro cytotoxicity tests were performed on extracts from polymer films based on the ISO 10993-5 protocol. For film preparation, 8 mm × 8 mm glass slides were sonicated in acetone and isopropyl alcohol, followed by ozone plasma treatment for 15 minutes. Stock solutions of each polymer in DI H₂O (20 mg mL⁻¹) with 1 wt% (3glycidyloxypropyl)trimethoxysilane (GOPs) were spin-coated onto the glass substrates at 1200 rpm and heated at 140 °C for 30 minutes. Before performing cytotoxicity experiments, films were washed with ethanol and phosphate buffered saline (PBS) under agitated shaking. The following protocol was followed to perform the live/dead assay.³¹ L929 Cells (derivative of Strain L- Connective mouse tissue) were obtained from ATCC (Cat no. CCL-1) and cultured in Dulbecco's Modified Eagle's Medium (DMEM)-high glucose media (Corning; Cat no. 10-013-CV) supplemented with both 10% fetal bovine serum (FBS) and 1% antibiotic-antimycotic directly on the polymer coated glass slides within a 24-well polystyrene tissue culture plate. The plate was incubated at 37 °C with 5% CO₂ in a humidified incubator for 24 hours. A live/dead solution was prepared with 0.5 µL calcein AM, 2.0 µL ethidium homodimer (EthD-1), and 1.0 μL of Hoechst in 1 mL of media. Each film was stained with live/dead solution (400 μL), incubated for 30 minutes, and imaged after destaining. Cell viability percentage was calculated using matlab R2021B.

The following protocol was followed to perform 3-(4,5-dimethylthiazol-2-yl)-2,5diphenyltetrazolium bromide (MTT) assay.³² DMEM media was added directly onto the polymer coated glass slides within a 24-well polystyrene tissue culture plate. Media was also added onto glass slide without a polymer coating as a control. The plate was incubated at 37 °C with 5% CO₂ in a humidified incubator for 24 hours to create extract media. Separately, a suspension of L929 cells was prepared at a concentration of 4×10^4 cell mL⁻¹ and $100 \ \mu L$ of the suspension was dispensed into a 96 well plate. The plate was incubated at 37 °C with 5% CO₂ in a humidified incubator for 24 hours. After 24 hours culture media was removed from the wells and replaced by 50 µL of extract media from a polymer film and 50 µL of culture media. The control had "extract media" from the glass surface without a polymer film. For a positive control, media was replaced with 20% DMSO (prepared in culture media) that causes severe cell death. For a negative control 100 µL of culture media was used but with no cells, and the blank contained 100 µL extract media, but with no cells. Following 48 hours and 72 hours the extract media and culture media were replaced by fresh 100 µL culture media, in their respective wells, to which 10 µL of 12 mM MTT was added. Plates were incubated in dark environment for 4 hours, followed by the addition of 100 µL of the SDS-HCL solution to each well and thorough mixing. Plates were incubated at 37 °C for 8 hours, mixed thoroughly, and the absorbance was measured at 570 nm using UV-Vis spectroscopy. MTT assays were repeated in a triplicate.

2.8 Hemocompatibility assay. 12 mL of the blood samples were collected from three female rabbits and pooled together in anticoagulant vials. Stock solutions of the polymers in DI water were prepared in the following concentrations: 15 mg mL⁻¹, 10 mg mL⁻¹ and 5 mg mL⁻¹. The protocol to perform the hemolysis assays were adapted from prior literature procedures. ³³⁻³⁴ Briefly, 300 μL of polymer solution was added to 4 mL of 0.9% saline solution and equilibrated

for 30 min at 37 °C. 200 μL of diluted blood (4 mL blood diluted in 5 mL of 0.9% saline solution) was added to each polymer extract. A negative control was prepared by adding 200 μL of diluted blood to 4 mL of 0.9% saline solution (0% hemolysis) and a positive control was prepared by adding 200 μL of diluted blood to 4 mL of DI water (100% hemolysis). Each sample was then incubated at 37 °C for 1 hour, centrifuged at 1000 rpm for 5 minutes and the absorbance of the supernatant was measured at 545 nm. Blank solutions with corresponding polymer concentrations were used to subtract polymer absorption at 545 nm from the measured experimental absorbance for each condition. All the hemolysis experiments were performed in a triplicate.

2.9 Biomaterial Functionalization. Gelatin type A (gel strength 300) was dissolved in Dulbecco's phosphate-buffered saline (DPBS, 1 g/ 50 mL) and the mixture was stirred at 55 °C until homogenous. Each polymer was individually dissolved in DPBS and added dropwise to the gelatin solution to obtain mixtures of varying mass ratios (2 %, 5 %, and 10 %). Each solution was incubated with stirring overnight at 55 °C. The modified gelatin solutions were then cooled to allow for gel formation. After gelation the samples were broken apart into small pieces and washed with DI H₂O. Samples were lyophilized for 72 h (Freezone 6, Labconco) before analysis.

3. RESULTS AND DISCUSSION

3.1 PEDOT-NHS Synthesis and Characterization. Of the reported EDOT derivatives for biofunctionalization,^{20, 35} surface deposition via electropolymerization remains the polymerization method of choice,³⁶⁻³⁹ precluding water-processible materials and solution processing of biomaterials. Recently direct (hetero)arylation polymerization (DHAP) has been utilized as a tool to develop anionic, water processible copolymers with opto(electronic) properties analogous to those synthesized through chemical oxidative polymerization.^{26, 30} Using

the reported DHAP methodology, **PEDOT-S** derivatives with handles for post-functionalization were synthesized by leveraging a N-Hydroxysuccinimide (NHS) activated EDOT monomer (EDOT-NHS, Scheme 1a) synthesized from previously reported 2-aminomethyl EDOT (EDOT-NH₂). EDOT-NHS was statistically incorporated (10 mol%) into PEDOT-S via DHAP to afford the copolymer poly[(EDOT-NHS)-co-(EDOT-S)] (PEDOT-NHS-10) (Scheme 1b). To investigate the impact of EDOT-NHS loading, an alternating copolymer was also synthesized (PEDOT-NHS-50). The DHAP methodology was utilized rather than other chemical oxidative polymerization pathways reported for anionic PEDOT derivatives, as it provides relatively high molecular weight (> 12 monomer units),³⁰ and is iron-free, thus preventing the introduction of known toxicants. Each polymer was purified utilizing 3 kDa MWCO dialysis bags, confirming high molecular weight formation compared to more commonly performed iron-catalyzed protocols. ¹H NMR (D₂O) measurements of each material were carried out showing broad peaks in agreement with previous reports of anionic PEDOT derivatives. 18, 26, 30 Poor resolution in this class of materials can be rationalized by a Knight shift, where NMR line shift and broadening manifest from an increase in the Pauli paramagnetic spin susceptibility. 40 Unlike PEDOT:PSS, and materials synthesized via electropolymerization, each of the reported materials demonstrate aqueous solubility at > 20 mg mL⁻¹(Figure S1), enabling simplified processing at relatively high concentrations of polymer.

The optical properties of both **PEDOT-NHS-10** and **PEDOT-NHS-50** are also consistent with that of **PEDOT-S** in both the pristine and oxidized state (**Figure 1a**).²⁶ The absorption spectrum of the neutral chain is characterized by a strong peak in the visible range due to the $\pi \to \pi^*$ transition, and broad absorption bands at wavelengths > 800 nm are typical for polaronic and bipolaronic states. Consistent with self-doped anionic PEDOT derivatives, pristine PEDOT-NHS

materials are partially oxidized. As previously demonstrated with PEDOT-S, both PEDOT-NHS-10 and PEDOT-NHS-50 can be further oxidized chemically or electrochemically. 15, 26 As a representative example, PEDOT-NHS-10 was further oxidized using ammonium persulfate (APS), which is confirmed by the complete suppression of the $\pi \to \pi^*$ transition (Figure 1b). Similarly, both polymers were able to be completely doped and dedoped electrochemically (Figure 1c, Figure S2), suggesting that the incorporation of EDOT-NHS structural units do not dramatically alter the optical behavior of PEDOT-S, regardless of loading. PEDOT-NHS-10 was also tested as a channel within an organic electrochemical transistor (OECT), a three terminal device commonly used in bioelectronic applications (Figure S8). 1, 41-42 The channel was immersed within a common ionic liquid electrolyte ([EMIM][TFSI]) to avoid **PEDOT-NHS-10** solvation during operation. Upon the application of $V_{\rm GS} < 0$ V, an increase in the channel current was observed. This accumulation-mode behavior has been observed in other OECTs fabricated with PEDOT-S,⁴³⁻⁴⁵ as well as other anionic conjugated polyelectrolytes.⁴⁶ X-ray photoelectron spectroscopy (XPS) analysis of the device fabricated with PEDOT-NHS-10 shows a single band at 398.4 eV in the N(1s) binding energy region (Figure S9), which is diagnostic of the nitrogen within the NHS functional handle.⁴⁷ Therefore, PEDOT-NHS copolymers can act as active materials for bioelectronic applications while presenting surface functionality for subsequent modification. Future optimization through materials processing or active material blending can be explored to utilize these materials within biosensing applications. 35, 45

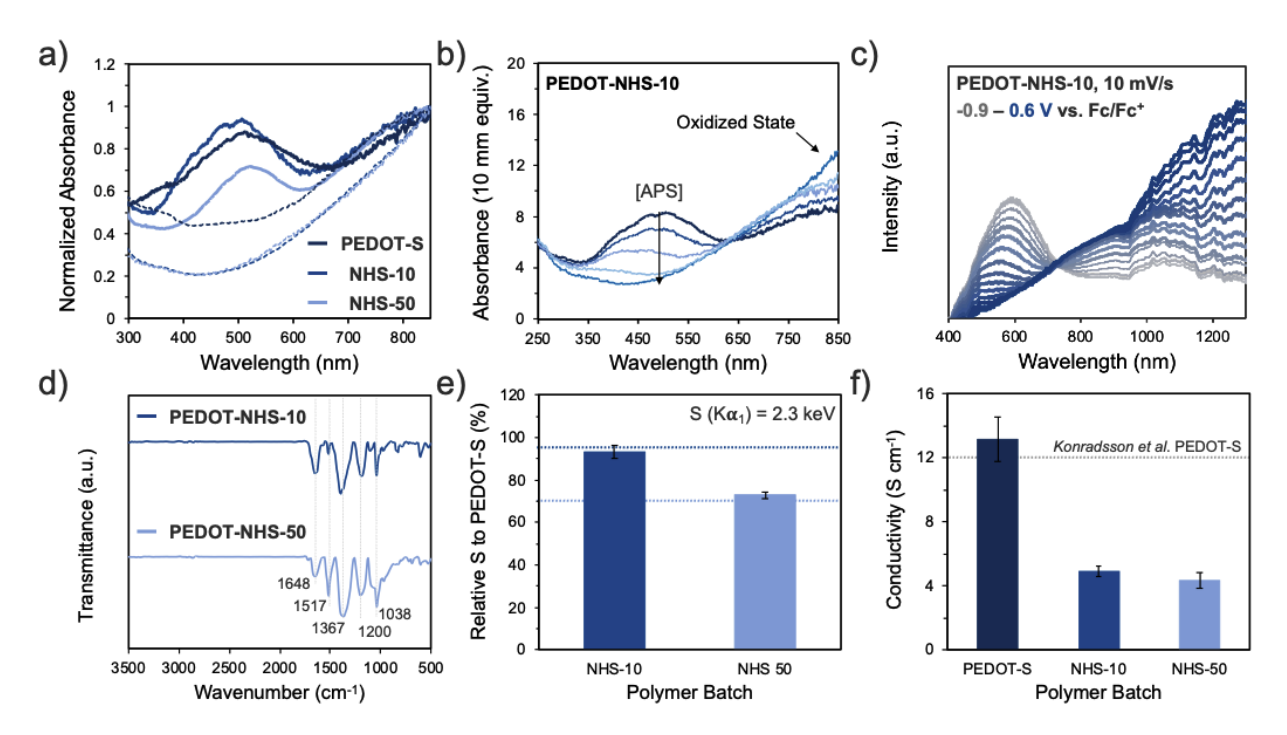


Figure 1. UV-vis spectrum of PEDOT-S, PEDOT-NHS-10, and PEDOT-NHS-50 in their (a) pristine (solid line) and oxidized state (dotted line). (b) UV-vis spectrum of PEDOT-NHS-10 upon chemical doping with aqueous APS solution. (c) Spectroelectrochemical measurements of PEDOT-NHS-10. Measurements were taken with 10 mV increments, with films deposited on indium tin oxide (ITO) electrodes). (d) ATR-FTIR spectra of PEDOT-NHS-10 and PEDOT-NHS-50. (e) Relative sulfur within PEDOT-NHS-10 and PEDOT-NHS-50 relative to PEDOT-S obtained through XRF analysis. (f) Four-point probe measurements for each material.

ATR-FTIR analysis of PEDOT-NHS copolymers displays characteristic bands for PEDOT-based materials (**Figure 1d**).¹⁷ Bands at 1517 and 1367 cm⁻¹ are attributed to C=C and C-C stretching vibrations of the thiophene ring, respectively, and the C-O-C stretching vibration of the ethylenedioxy group can be observed at 1200 cm⁻¹. Characteristic vibrations of the NHS lactam at ~1648 cm⁻¹ were observed, confirming EDOT-NHS incorporation into both copolymers. With increased loading of EDOT-NHS, the shift at 1517 cm⁻¹ was relatively stronger in PEDOT-NHS 50 which may be attributed to elevated N-H bending from the secondary amide which attaches the NHS side chain overlapping with the C=C stretching from the polymer backbone. Characteristic S=O stretching vibrations were also observed from the

sulfonate salts at 1038 cm⁻¹.⁴⁸ Elemental analysis of both materials was performed to determine the amount of EDOT-NHS incorporation within each polymer. X-ray fluorescence (XRF) was used to quantify relative sulfur content between PEDOT-S, PEDOT-NHS-10, and PEDOT-NHS-50 (Figure 1e). As the PEDOT-NHS copolymers have relatively less sulfur within each constitutional repeating unit compared to PEDOT-S, comparison of the mass normalized fluorescence of the $K_{\alpha l}$ transition for sulfur at ~2.3 keV of each material can be used to indirectly quantify incorporation of EDOT-NHS, via loss of EDOT-S structural units. The observed relative sulfur content of each polymer was within error of theory (Figure S3), confirming ~10% and ~50% EDOT-NHS incorporation within PEDOT-NHS-10 and PEDOT-NHS-50, respectively.

Previous reports of **PEDOT-S** and structural analogues have demonstrated conductivities ranging from ~ 0.1 - 40 S cm⁻¹, depending on the polymer structure and synthesis protocol.^{26, 43} **PEDOT-S** synthesized via DHAP demonstrated a conductivity of 13.2 ± 1.4 S cm⁻¹, which is within error to the original report by Konradsson *et al.*¹⁸ Both **PEDOT-NHS-10** and **PEDOT-NHS-50** had lower conductivities of 4.9 ± 0.3 S cm⁻¹ and 4.3 ± 0.5 S cm⁻¹, respectively, but higher conductivity than other reports of **PEDOT-S** (**Figure 1f**, **Table S1**). The relatively similar conductivity between the three materials is consistent with prior reports of sulfonated PEDOT-based copolymers, where the incorporation of hydrophobic comonomers did not show severe deleterious effects on electronic properties.²⁶ At both 10% and 50% EDOT-NHS incorporation, water soluble, electrically conductive polymers with available binding sites were achieved.

3.2 Biocompatibility of PEDOT-NHS. When designing materials for bioelectronic applications, it is important to assess biocompatibility, an often-overlooked property in organic electronics. For various synthetic design strategies to achieve biocompatibility in conjugated

polymers, we refer the reader elsewhere.¹¹ Following a modified ISO 10993-5 protocol, cytotoxicity was assessed against L929 cells using films of each material for live/dead analysis (**Figure 2a-b**) and extracts from the polymer films for MTT analysis (**Figure 2c**). As this protocol is designed to test the biocompatibility of the material under conditions most similar to that of the intended application, the films were crosslinked using GOPS, a common crosslinker for conjugated polyelectrolytes in bioelectronic applications.⁴⁶ The live/dead assay confirmed high viability percentage (>95%) of cells for each of the three materials (**Figure 2b, Figure S4**). Despite the good viability observed via live/dead analysis, clear differences in L929 cell spreading/adhesion are evident, which may be due to effects of film roughness, surface charge, or chemistry; this phenomenon is a subject for future investigation. Results from the colorimetric MTT assay after both 48 h and 72 h incubation are displayed in **Figure 2c**. All three materials did not show significant cytotoxicity as cell viability was greater than 80%.

Hemolysis testing was also performed as it provides a simple and reliable measure for estimating blood compatibility, an important material requirement for bioelectronic applications such as regenerative engineering or healthcare monitoring. Unlike live/dead and MTT analyses which investigate cell viability in direct contact with the polymer films and extracts from the films, respectively, hemolysis was performed on aqueous solutions of each polymer to represent an extreme scenario. Each solution demonstrated little evidence of hemolysis (< 4 %, Figure 2d, Figure S5) and can therefore be considered highly hemocompatible; particularly as such high concentrations are well beyond what would be used in a bioelectronic application. As observed with the cell viability assessment, greater incorporation of EDOT-NHS structural units within the polymer backbone, and higher concentrations demonstrated relatively lower hemocompatiblity. It is not clear why increased concentrations of NHS functionalities may decrease cell viability

and hemocompatibility, as such chemistries are commonly utilized in biomaterial applications.⁴⁹ Chemical reactions between the NHS groups and amines present within the cell membrane may explain the relative decrease in biocompatibility. However, such effects appeared relatively small as each material demonstrated good biocompatibility, even at high concentrations suggesting potential for future bioelectronic applications.

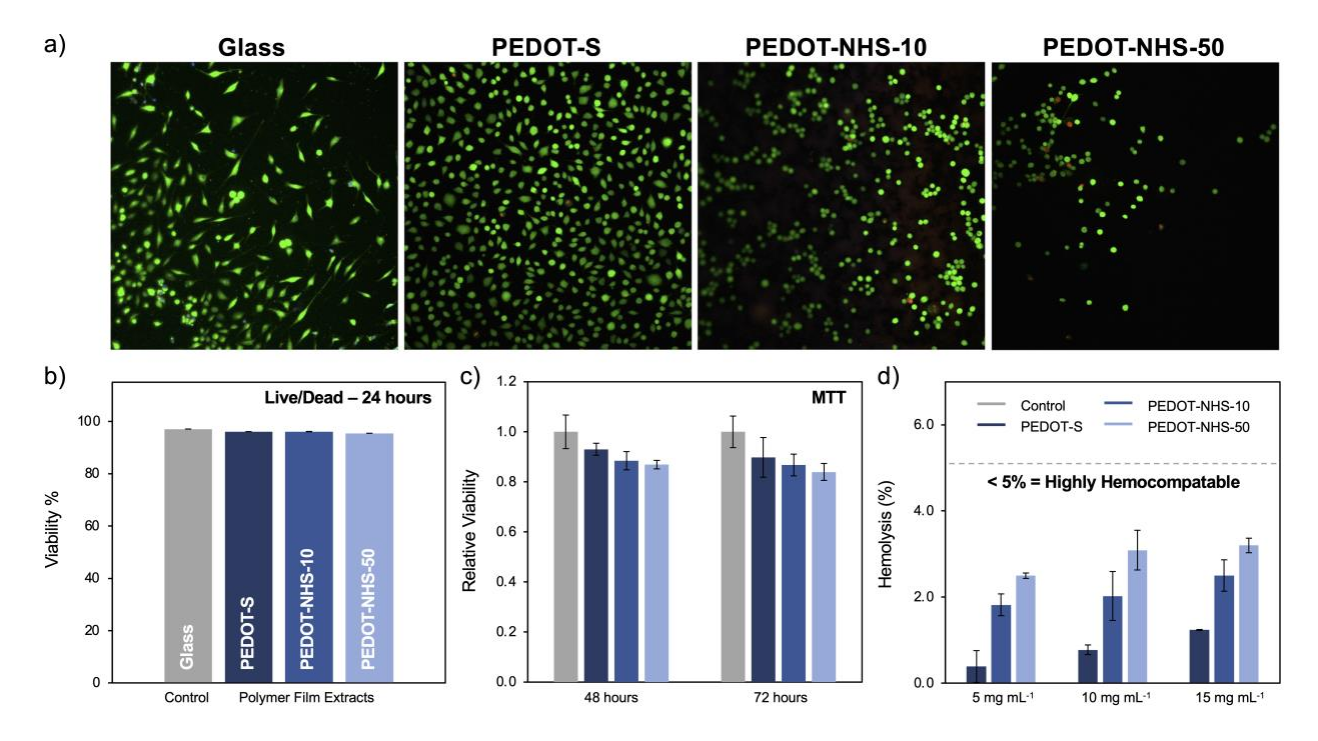


Figure 2. (a) Fluorescent images of cells taken after live/dead assay, where calcein AM (green) represents live cells, and ethidium homodimer (red) represents dead cells in contact with films of each polymer. (b) Quantitative measurement of cell viability using live/dead assay. (c) Cell viability of L929 cells treated with either media alone or film extracts of **PEDOT-NHS 50** after incubation for 48 h and 72 h. (d) Percent hemolysis of each polymer at 5 mg mL⁻¹, 10 mg mL⁻¹ and 15 mg mL⁻¹ concentrations.

3.3 Biofunctionalization via PEDOT-NHS copolymers. Many conductive polymers such as **PEDOT-S** and **PEDOT:PSS** have been incorporated into biomaterials for various bioelectronic applications, ^{15, 22, 43, 50} however their lack of chemical handles for functionalization has required the use of rudimentary blending and soaking procedures. ^{35, 51} The physical entrapment of

conductive polymers within a biomaterial, rather than chemical binding, allows for potential loss of the polymer over time and therefore decreased bioelectronic performance or increased toxicity to the cellular environment. Relatively low loadings of EDOT-NHS structural units were targeted within the PEDOT-NHS copolymers (10% and 50%) to support biofunctionalization via amidation of the activated NHS-ester, while minimizing the loss of alkyl sulfonate groups required to self-dope the polymer.

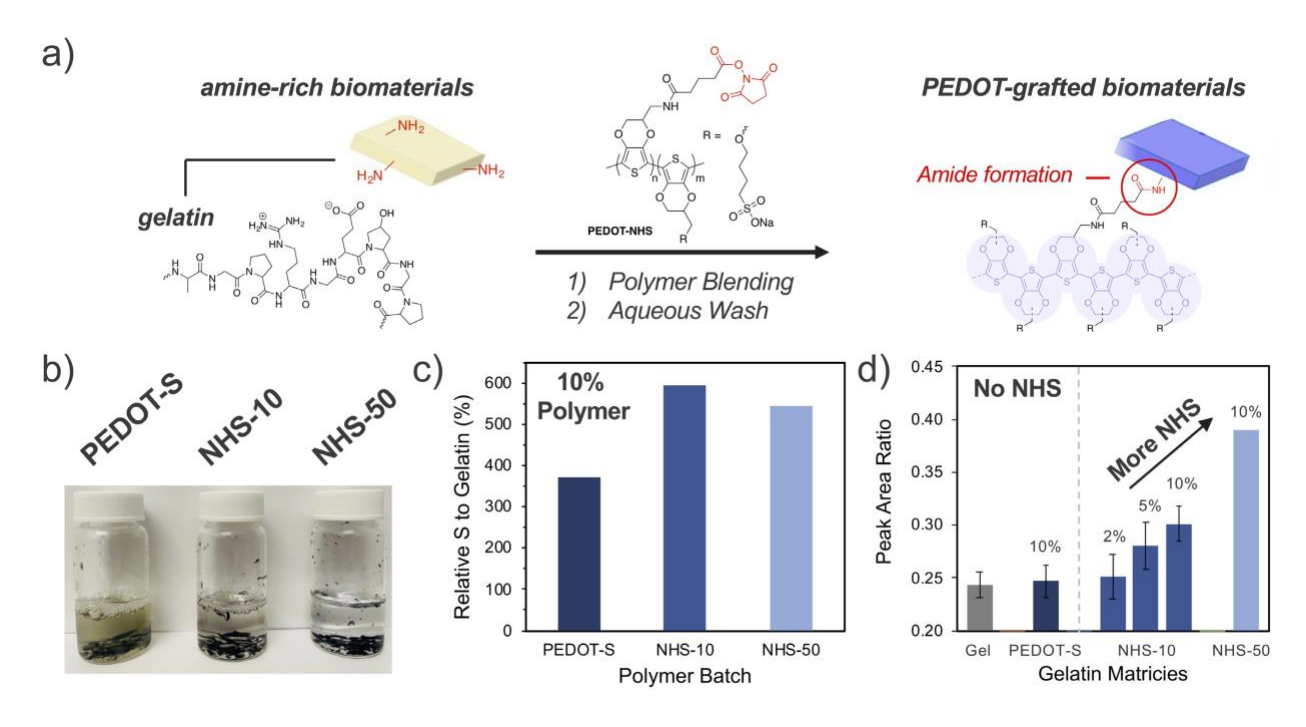


Figure 3. (a) Pictorial representation of the functionalization of amine-rich biomaterials such as gelatin with PEDOT-NHS copolymers. (b) Image demonstrating leeching of **PEDOT-S** from the gelatin hydrogel and the absence of leaching with corresponding PEDOT-NHS incorporated gels. after incubation demonstrating a lack of hemolytic reaction. (C) Relative sulfur within **PEDOT-S**, **PEDOT-NHS-10**, and **PEDOT-NHS-50** gelatin samples compared to a gelatin control without added polymer. (d) ATR-FTIR peak area ratios of amide I/amide A band of gelatin matrices with different concentrations of PEDOT-NHS copolymer and PEDOT-S without a functional handle for covalent binding.

To demonstrate the utility of these chemical handles, gelatin, a common biomaterial used for tissue engineering applications,^{7, 52} was modified with **PEDOT-S**, **PEDOT-NHS-10**, and

PEDOT-NHS 50 using a simple blending approach (Figure 3a). Gelatin solutions in DPBS were first stirred at elevated temperatures with respective aqueous polymer solutions. DPBS was utilized as the reaction between NHS esters of the polymers, and primary amines of the gelatin, requires slightly alkaline conditions to yield stable amide bonds. Upon cooling, soft homogenous gels were formed, broken apart and washed with excess water to remove unbound polymer. Only the supernatant from gels blended with PEDOT-S were blue, suggesting that only the PEDOT-NHS copolymers bound to the gelatin as intended (Figure 3b). In fact, the PEDOT-S incorporated gel had to be washed with > 200 mL of DI H₂O to get a visibly clear supernatant, compared to the supernatants of PEDOT-NHS incorporated materials which lacked color upon initial washing. Similarly, when dried, the gelatin sample with incorporated PEDOT-S was lighter in color than those with incorporated PEDOT-NHS copolymers (Figure S6). XRF was used to quantify relative sulfur content between dried gelatin samples with 10% loading by mass of each of the three polymers. When compared to a similarly prepared gelatin sample without blended conjugated polymer, elevated sulfur content was observed for each sample (Figure 3c). As previously mentioned, PEDOT-S has more sulfur per unit mass than both PEDOT-NHS copolymers (Figure S3), therefore if the same amount of each polymer was maintained within the gelatin samples after washing, we would anticipate more sulfur in the PEDOT-S incorporated gelatin composite. However, the opposite was observed as the amount of sulfur detected in the PEDOT-S incorporated gelatin sample was much lower than those with the PEDOT-NHS copolymers, suggesting significant loss of **PEDOT-S** during the water wash. The elevated sulfur observed in the gelatin samples containing PEDOT-NHS copolymers suggests (1) successful binding between the amine groups of the gelatin and the NHS groups of the copolymers and (2) 10% EDOT-NHS incorporation was sufficient to prevent diffusive loss from

the biomaterial. While it is difficult to quantify exactly whether PEDOT-NHS-10 or PEDOT-NHS-50 was better maintained within the gelatin composite, the slightly darker hue of the PEDOT-NHS-50 incorporated composite (Figure S6), and the relatively similar sulfur content between the two PEDOT-NHS incorporated composites (despite the significantly diminished sulfur content in PEDOT-NHS-50 vs. PEDOT-NHS-10) suggests PEDOT-NHS-50 was better incorporated.

To verify binding occurred via NHS ester reaction, gelatin samples containing either PEDOT-S, PEDOT-NHS-10, or PEDOT-NHS-50 were investigated using attenuated total reflectance Fourier transform infrared spectroscopy (ATR-FTIR). The spectra of unmodified gelatin and gelatin cross-linked using PEDOT-NHS are shown in Figure S7. Characteristic amide bonds are present after crosslinking, suggesting the structure of gelatin is maintained (amide A: ~3500 – 3200 cm⁻¹, amide B: \sim 3000 cm⁻¹, amide I: \sim 1635 cm⁻¹, amide II: \sim 1550 cm⁻¹, amide III: \sim 1240 cm⁻¹).⁵³⁻⁵⁴ Crosslinking occurs by reacting free -NH₂ groups (~3300 cm⁻¹) to form a -CONHbond (~1635 cm⁻¹), therefore increasing the intensity of the amide I band while decreasing that of amide A.55 The peak area of the amide I band to that of the amide A band was determined, and their ratio was plotted as a function of the concentration of polymer incorporation (Figure 3d). The increase in the peak area ratios with increased loading of EDOT-NHS is consistent with increased covalent binding. No significant change in peak area ratio was observed with increased loading of PEDOT-S compared to that of gelatin, suggesting a lack of binding. Taken together, incorporation of the **EDOT-NHS** within the conjugated polyelectrolyte biofunctionalization via amidation, and therefore covalent modification of protein-based biomaterials.

4. CONCLUSIONS

In summary, the incorporation of NHS groups within a prototypical conjugated polyelectrolyte **PEDOT-S** can afford polymers with water solubility, conductivity, biocompatibility, and handles for biofunctionalization, a rare demonstration. Our results suggest that low loadings of EDOT-NHS were required to achieve these properties, as **PEDOT-NHS-10** and **PEDOT-NHS-50** both had similar conductivity and biomaterial immobilization. Lower loadings of EDOT-NHS within the polymer also afforded greater biocompatibility and hemocompatibility, suggesting minimal incorporation is beneficial. While gelatin was used to demonstrate biofunctionalization, the amine reactive NHS-ester can be bound to other biomaterials utilized for bioelectronics and regenerative engineering such as collagen, silk, keratin, chitosan, etc. These handles can also be leveraged for bioconjugation of biomacromolecules or signaling agents for various sensing applications.

The reported synthetic strategy is highly tunable, as a variety of monomers bearing other chemistries for postmodification can be utilized to generate conjugated polymers and polyelectrolytes for bioelectronic applications.^{20, 48, 56} These results build upon the growing literature of designing conductive polymers for biomaterial incorporation and lay the groundwork for an extension of PEDOT-NHS copolymers into regenerative engineering, sensing, and other bioelectronic applications.

ASSOCIATED CONTENT

The Supporting Information is available free of charge on the ACS Publications website.

Details of solubility experiments; spectroelectrochemical characterization; theoretical relative sulfur calculations; conductivity analysis; and OECT characterization (PDF)

AUTHOR INFORMATION

Corresponding Author

* Jonathan Rivnay – Department of Biomedical Engineering, Northwestern University,
Evanston, Illinois 60208, United States; Simpson Querrey Institute, Northwestern University,
Chicago, Illinois 60611, United States; orcid.org/0000- 0002-0602-6485; Email:

jrivnay@northwestern.edu

ACKNOWLEDGMENT

J. T. was primarily supported by an ONR YIP (SP0056955). J. R. gratefully acknowledges support from the Alfred P. Sloan Foundation (FG-2019-12046). This work made use of the IMSERC X-RAY facility at Northwestern University, which has received support from the Soft and Hybrid Nanotechnology Experimental (SHyNE) Resource (NSF ECCS-2025633), and Northwestern University. This work made use of the IMSERC NMR facility at Northwestern University, which has received support from the Soft and Hybrid Nanotechnology Experimental (SHyNE) Resource (NSF ECCS-2025633), Int. Institute of Nanotechnology, and Northwestern University. Conductivity measurements were performed in the Materials Characterization and Imaging (MatCI) Facility, which receives support from the NSF MRSEC Program (NSF DMR-1720139). FTIR measurements utilized the Keck-II facility of Northwestern University's NUANCE Center, which has received support from the SHyNE Resource (NSF ECCS-2025633), the IIN, and Northwestern's MRSEC program (NSF DMR-1720139).

REFERENCES

- 1. Inal, S.; Rivnay, J.; Suiu, A.-O.; Malliaras, G. G.; McCulloch, I., Conjugated Polymers in Bioelectronics. *Acc. Chem. Res.* **2018**, *51*, 1368-1376.
- 2. Higgins, S. G.; Lo Fiego, A.; Patrick, I.; Creamer, A.; Stevens, M. M., Organic Bioelectronics: Using Highly Conjugated Polymers to Interface with Biomolecules, Cells, and Tissues in the Human Body. *Adv. Mater. Technol.* **2020**, *5*, 2000384.
- 3. Ohayon, D.; Inal, S., Organic Bioelectronics: From Functional Materials to Next-Generation Devices and Power Sources. *Adv. Mater* **2020**, *32*, 2001439.
- 4. Zhao, S.; Mehta, A. S.; Zhao, M., Biomedical applications of electrical stimulation. *Cell Mol Life Sci* **2020,** 77, 2681-2699.
- 5. Mehta, A. S.; Ha, P.; Zhu, K.; Li, S.; Ting, K.; Soo, C.; Zhang, X.; Zhao, M., Physiological electric fields induce directional migration of mammalian cranial neural crest cells. *Dev Biol* **2021**, *471*, 97-105.
- 6. Van Vlierberghe, S.; Dubruel, P.; Schacht, E., Biopolymer-Based Hydrogels As Scaffolds for Tissue Engineering Applications: A Review. *Biomacromolecules* **2011**, *12*, 1387-1408.
- 7. Wang, C.; Yokota, T.; Someya, T., Natural Biopolymer-Based Biocompatible Conductors for Stretchable Bioelectronics. *Chem. Rev.* **2021**, *121*, 2109-2146.
- 8. Fu, F.; Wang, J.; Zeng, H.; Yu, J., Functional Conductive Hydrogels for Bioelectronics. *ACS Materials Lett.* **2020,** *2*, 1287-1301.
- 9. Petty, A. J.; Keate, R. L.; Jiang, B.; Ameer, G. A.; Rivnay, J., Conducting Polymers for Tissue Regeneration in Vivo. *Chem. Mater.* **2020**, *32*, 4095-4115.
- 10. Chiong, J. A.; Tran, H.; Lin, Y.; Zheng, Y.; Bao, Z., Integrating Emerging Polymer Chemistries for the Advancement of Recyclable, Biodegradable, and Biocompatible Electronics. *Adv. Sci.* **2021**, *8*, 2101233.
- 11. Tropp, J.; Rivnay, J., Design of biodegradable and biocompatible conjugated polymers for bioelectronics. *J. Mater. Chem. C* **2021**, *9*, 13543-13556.
- 12. Balint, R.; Cassidy, N. J.; Cartmell, S. H., Conductive polymers: Towards a smart biomaterial for tissue engineering. *Acta Biomater.* **2014**, *10*, 2341-2353.
- 13. Talikowska, M.; Fu, X.; Lisak, G., Application of conducting polymers to wound care and skin tissue engineering: A review. *Biosens. Bioelectron.* **2019**, *135*, 50-63.
- 14. Guo, B.; Ma, P. X., Conducting Polymers for Tissue Engineering. *Biomacromolecules* **2018**, *19*, 1764-1782.
- 15. Keate, R. L.; Tropp, J.; Serna, C.; Rivnay, J., A Collagen-Conducting Polymer Composite with Enhanced Chondrogenic Potential. *Cel. Mol. Bioeng.* **2021**, *14*, 501-512.
- 16. Donahue, M. J.; Sanchez-Sanchez, A.; Inal, S.; Qu, J.; Owens, R. M.; Mecerreyes, D.; Malliaras, G. G.; Martin, D. C., Tailoring PEDOT properties for applications in bioelectronics. *Mater. Sci. Eng. R Rep.* **2020**, *140*, 100546.
- 17. Minudri, D.; Mantione, D.; Dominguez-Alfaro, A.; Moya, S.; Maza, E.; Bellacanzone, C.; Antognazza, M. R.; Mecerreyes, D., Water Soluble Cationic Poly(3,4-Ethylenedioxythiophene) PEDOT-N as a Versatile Conducting Polymer for Bioelectronics. *Adv. Electron. Mater.* **2020**, *6*, 2000510.
- 18. Karlsson, R. H.; Herland, A.; Hamedi, M.; Wigenius, J. A.; Åslund, A.; Liu, X.; Fahlman, M.; Inganäs, O.; Konradsson, P., Iron-Catalyzed Polymerization of Alkoxysulfonate-Functionalized 3,4-Ethylenedioxythiophene Gives Water-Soluble Poly(3,4-ethylenedioxythiophene) of High Conductivity. *Chem. Mater.* **2009**, *21*, 1815-1821.

- 19. Istif, E.; Mantione, D.; Vallan, L.; Hadziioannou, G.; Brochon, C.; Cloutet, E.; Pavlopoulou, E., Thiophene-Based Aldehyde Derivatives for Functionalizable and Adhesive Semiconducting Polymers. *ACS Appl. Mater. Interfaces* **2020**, *12*, 8695-8703.
- 20. Mantione, D.; Del Agua, I.; Sanchez-Sanchez, A.; Mecerreyes, D., Poly(3,4-ethylenedioxythiophene) (PEDOT) Derivatives: Innovative Conductive Polymers for Bioelectronics. *Polymers* **2017**, *9*, 354.
- 21. Abedi, A.; Hasanzadeh, M.; Tayebi, L., Conductive nanofibrous Chitosan/PEDOT:PSS tissue engineering scaffolds. *Mater. Chem. Phys.* **2019**, *237*, 121882.
- 22. Guex, A. G.; Puetzer, J. L.; Armgarth, A.; Littmann, E.; Stavrinidou, E.; Giannelis, E. P.; Malliaras, G. G.; Stevens, M. M., Highly porous scaffolds of PEDOT:PSS for bone tissue engineering. *Acta Biomater.* **2017**, *62*, 91-101.
- 23. Sirivisoot, S.; Pareta, R.; Harrison, B. S., Protocol and cell responses in three-dimensional conductive collagen gel scaffolds with conductive polymer nanofibres for tissue regeneration. *Interface Focus* **2014**, *4*, 20130050.
- 24. Dauzon, E.; Mansour, A. E.; Niazi, M. R.; Munir, R.; Smilgies, D.-M.; Sallenave, X.; Plesse, C.; Goubard, F.; Amassian, A., Conducting and Stretchable PEDOT:PSS Electrodes: Role of Additives on Self-Assembly, Morphology, and Transport. *ACS Appl. Mater. Interfaces* **2019**, *11*, 17570-17582.
- 25. Kayser, L. V.; Lipomi, D. J., Stretchable Conductive Polymers and Composites Based on PEDOT and PEDOT:PSS. *Adv. Mater.* **2019**, *31*, 1806133.
- 26. Beaumont, C.; Turgeon, J.; Idir, M.; Neusser, D.; Lapointe, R.; Caron, S.; Dupont, W.; D'Astous, D.; Shamsuddin, S.; Hamza, S.; Landry, É.; Ludwigs, S.; Leclerc, M., Water-Processable Self-Doped Conducting Polymers via Direct (Hetero)arylation Polymerization. *Macromolecules* **2021**, *54*, 5464-5472.
- 27. Yano, H.; Kudo, K.; Marumo, K.; Okuzaki, H., Fully soluble self-doped poly(3,4-ethylenedioxythiophene) with an electrical conductivity greater than 1000 S cm-1. *Sci. Adv. 5*, eaav9492.
- 28. Hai, W.; Goda, T.; Takeuchi, H.; Yamaoka, S.; Horiguchi, Y.; Matsumoto, A.; Miyahara, Y., Specific Recognition of Human Influenza Virus with PEDOT Bearing Sialic Acid-Terminated Trisaccharides. *ACS Appl. Mater. Interfaces* **2017**, *9*, 14162-14170.
- 29. Haraguchi, S.; Tsuchiya, Y.; Shiraki, T.; Sada, K.; Shinkai, S., Control of polythiophene redox potentials based on supramolecular complexation with helical schizophyllan. *Chem. Commun.* **2009**, (40), 6086-6088.
- 30. Ayalew, H.; Wang, T.-l.; Wang, T.-H.; Hsu, H.-F.; Yu, H.-h., Direct C–H Arylation Polymerization to form Anionic Water-Soluble Poly(3,4-ethylenedioxythiophenes) with Higher Yields and Molecular Weights. *Synlett* **2018**, *29*, 2660-2668.
- 31. Krauss, G.; Meichsner, F.; Hochgesang, A.; Mohanraj, J.; Salehi, S.; Schmode, P.; Thelakkat, M., Polydiketopyrrolopyrroles Carrying Ethylene Glycol Substituents as Efficient Mixed Ion-Electron Conductors for Biocompatible Organic Electrochemical Transistors. *Adv. Funct. Mater.* **2021**, *31*, 2010048.
- 32. Ozdemir, K. G.; Yilmaz, H.; Yilmaz, S., In vitro evaluation of cytotoxicity of soft lining materials on L929 cells by MTT assay. *J Biomed Mater Res B Appl Biomater* **2009**, *90*, 82-86.
- 33. Mehta, A. S.; Singh, B. K.; Singh, N.; Archana, D.; Snigdha, K.; Harniman, R.; Rahatekar, S. S.; Tewari, R. P.; Dutta, P. K., Chitosan silk-based three-dimensional scaffolds containing gentamicin-encapsulated calcium alginate beads for drug administration and blood compatibility. *J Biomater Appl* **2015**, *29*, 1314-25.

- 34. Wang, X.; Gu, X.; Yuan, C.; Chen, S.; Zhang, P.; Zhang, T.; Yao, J.; Chen, F.; Chen, G., Evaluation of biocompatibility of polypyrrole in vitro and in vivo. *J Biomed Mater Res A* **2004**, *68*, 411-22.
- 35. Fenoy, G. E.; Azzaroni, O.; Knoll, W.; Marmisollé, W. A., Functionalization Strategies of PEDOT and PEDOT:PSS Films for Organic Bioelectronics Applications. *Chemosensors* **2021**, *9*, 212.
- 36. Luo, S.-C.; Mohamed Ali, E.; Tansil, N. C.; Yu, H.-h.; Gao, S.; Kantchev, E. A. B.; Ying, J. Y., Poly(3,4-ethylenedioxythiophene) (PEDOT) Nanobiointerfaces: Thin, Ultrasmooth, and Functionalized PEDOT Films with in Vitro and in Vivo Biocompatibility. *Langmuir* **2008**, *24*, 8071-8077.
- 37. Wu, B.; Cao, B.; Taylor, I. M.; Woeppel, K.; Cui, X. T., Facile Synthesis of a 3,4-Ethylene-Dioxythiophene (EDOT) Derivative for Ease of Bio-Functionalization of the Conducting Polymer PEDOT. *Front. Chem.* **2019**, *7*, 178.
- 38. Povlich, L. K.; Cho, J. C.; Leach, M. K.; Corey, J. M.; Kim, J.; Martin, D. C., Synthesis, copolymerization and peptide-modification of carboxylic acid-functionalized 3,4-ethylenedioxythiophene (EDOTacid) for neural electrode interfaces. *Biochim. Biophys. Acta Gen. Subj.* **2013**, *1830*, 4288-4293.
- 39. Ouyang, L.; Wei, B.; Kuo, C.-c.; Pathak, S.; Farrell, B.; Martin, D. C., Enhanced PEDOT adhesion on solid substrates with electrografted P(EDOT-NH2). *Sci. Adv.* **2017**, *3*, e1600448.
- 40. Yano, H.; Kudo, K.; Marumo, K.; Okuzaki, H., Fully soluble self-doped poly(3,4-ethylenedioxythiophene) with an electrical conductivity greater than 1000 S cm-1. *Sci. Adv.* **2019,** *5*, eaav9492.
- 41. Rivnay, J.; Inal, S.; Salleo, A.; Owens, R. M.; Berggren, M.; Malliaras, G. G., Organic electrochemical transistors. *Nat. Rev. Mater.* **2018**, *3*, 17086.
- 42. Paudel, P. R.; Tropp, J.; Kaphle, V.; Azoulay, J. D.; Lüssem, B., Organic electrochemical transistors from device models to a targeted design of materials. *J. Mater. Chem. C* **2021**, *9*, 9761-9790.
- 43. Mousa, A. H.; Bliman, D.; Hiram Betancourt, L.; Hellman, K.; Ekström, P.; Savvakis, M.; Strakosas, X.; Marko-Varga, G.; Berggren, M.; Hjort, M.; Ek, F.; Olsson, R., Method Matters: Exploring Alkoxysulfonate-Functionalized Poly(3,4-ethylenedioxythiophene) and Its Unintentional Self-Aggregating Copolymer toward Injectable Bioelectronics. *Chem. Mater.* **2022**, *34*, 2752-2763.
- 44. Musumeci, C.; Vagin, M.; Zeglio, E.; Ouyang, L.; Gabrielsson, R.; Inganäs, O., Organic electrochemical transistors from supramolecular complexes of conjugated polyelectrolyte PEDOTS. *J. Mater. Chem. C* **2019**, *7*, 2987-2993.
- 45. Zeglio, E.; Schmidt, M. M.; Thelakkat, M.; Gabrielsson, R.; Solin, N.; Inganäs, O., Conjugated Polyelectrolyte Blends for Highly Stable Accumulation-Mode Electrochemical Transistors. *Chem. Mater.* **2017**, *29*, 4293-4300.
- 46. Inal, S.; Rivnay, J.; Leleux, P.; Ferro, M.; Ramuz, M.; Brendel, J. C.; Schmidt, M. M.; Thelakkat, M.; Malliaras, G. G., A High Transconductance Accumulation Mode Electrochemical Transistor. *Adv. Mater.* **2014**, *26*, 7450-7455.
- 47. Lim, C. Y.; Owens, N. A.; Wampler, R. D.; Ying, Y.; Granger, J. H.; Porter, M. D.; Takahashi, M.; Shimazu, K., Succinimidyl Ester Surface Chemistry: Implications of the Competition between Aminolysis and Hydrolysis on Covalent Protein Immobilization. *Langmuir* **2014**, *30*, 12868-12878.

- 48. Williams, A. K.; Tropp, J.; Crater, E. R.; Eedugurala, N.; Azoulay, J. D., Thiol–Ene Click Post-Polymerization Modification of a Fluorescent Conjugated Polymer for Parts-per-Billion Pyrophosphate Detection in Seawater. *ACS Appl. Polym. Mater.* **2019**, *1*, 309-314.
- 49. Spicer, C. D.; Pashuck, E. T.; Stevens, M. M., Achieving Controlled Biomolecule–Biomaterial Conjugation. *Chem. Rev.* **2018**, *118*, 7702-7743.
- 50. Ryan, J. D.; Mengistie, D. A.; Gabrielsson, R.; Lund, A.; Müller, C., Machine-Washable PEDOT:PSS Dyed Silk Yarns for Electronic Textiles. *ACS Appl. Mater. Interfaces* **2017**, *9*, 9045-9050.
- 51. Bhat, M. A.; Rather, R. A.; Shalla, A. H., PEDOT and PEDOT:PSS conducting polymeric hydrogels: A report on their emerging applications. *Synth. Met.* **2021**, *273*, 116709.
- 52. Bello, A. B.; Kim, D.; Kim, D.; Park, H.; Lee, S. H., Engineering and Functionalization of Gelatin Biomaterials: From Cell Culture to Medical Applications. *Tissue Eng. Part B Rev.* **2020,** *26* (2), 164-180.
- 53. Skopinska-Wisniewska, J.; Tuszynska, M.; Olewnik-Kruszkowska, E., Comparative Study of Gelatin Hydrogels Modified by Various Cross-Linking Agents. *Materials* **2021**, *14*, 396.
- 54. Lee, D. H.; Arisaka, Y.; Tonegawa, A.; Kang, T. W.; Tamura, A.; Yui, N., Cellular Orientation on Repeatedly Stretching Gelatin Hydrogels with Supramolecular Cross-Linkers. *Polymers* **2019**, *11*, 2095.
- 55. Tiong, W. H. C.; Damodaran, G.; Naik, H.; Kelly, J. L.; Pandit, A., Enhancing Amine Terminals in an Amine-Deprived Collagen Matrix. *Langmuir* **2008**, *24*, 11752-11761.
- 56. Sun, H.; Schanze, K. S., Functionalization of Water-Soluble Conjugated Polymers for Bioapplications. *ACS Appl. Mater. Interfaces* **2022**, *14*, 20506-20519.

Table of Contents Graphic

